Journal Pre-proof

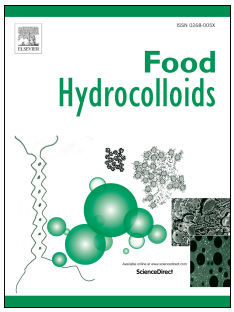

Effect of pre-printing gelatinization degree on the structure and digestibility of hot-extrusion 3D-printed starch

Bo Zheng, Yukuo Tang, Fengwei Xie, Ling Chen

PII: S0268-005X(21)00626-3

DOI: https://doi.org/10.1016/j.foodhyd.2021.107210

Reference: FOOHYD 107210

To appear in: *Food Hydrocolloids*

Received Date: 18 June 2021

Revised Date: 16 September 2021

Accepted Date: 21 September 2021

Please cite this article as: Zheng, B., Tang, Y., Xie, F., Chen, L., Effect of pre-printing gelatinization degree on the structure and digestibility of hot-extrusion 3D-printed starch, *Food Hydrocolloids*, https://doi.org/10.1016/j.foodhyd.2021.107210.

CRediT author statement:

Bo Zheng: Methodology, Validation, Formal analysis, Investigation, Data Curation, Writing - Original Draft, Visualization. **Yukuo Tang**: Methodology, Writing - Review & Editing. **Fengwei Xie**: Methodology, Resources, Writing - Review & Editing, Visualization. **Ling Chen:** Conceptualization, Methodology, Resources, Supervision, Project administration, Funding acquisition.

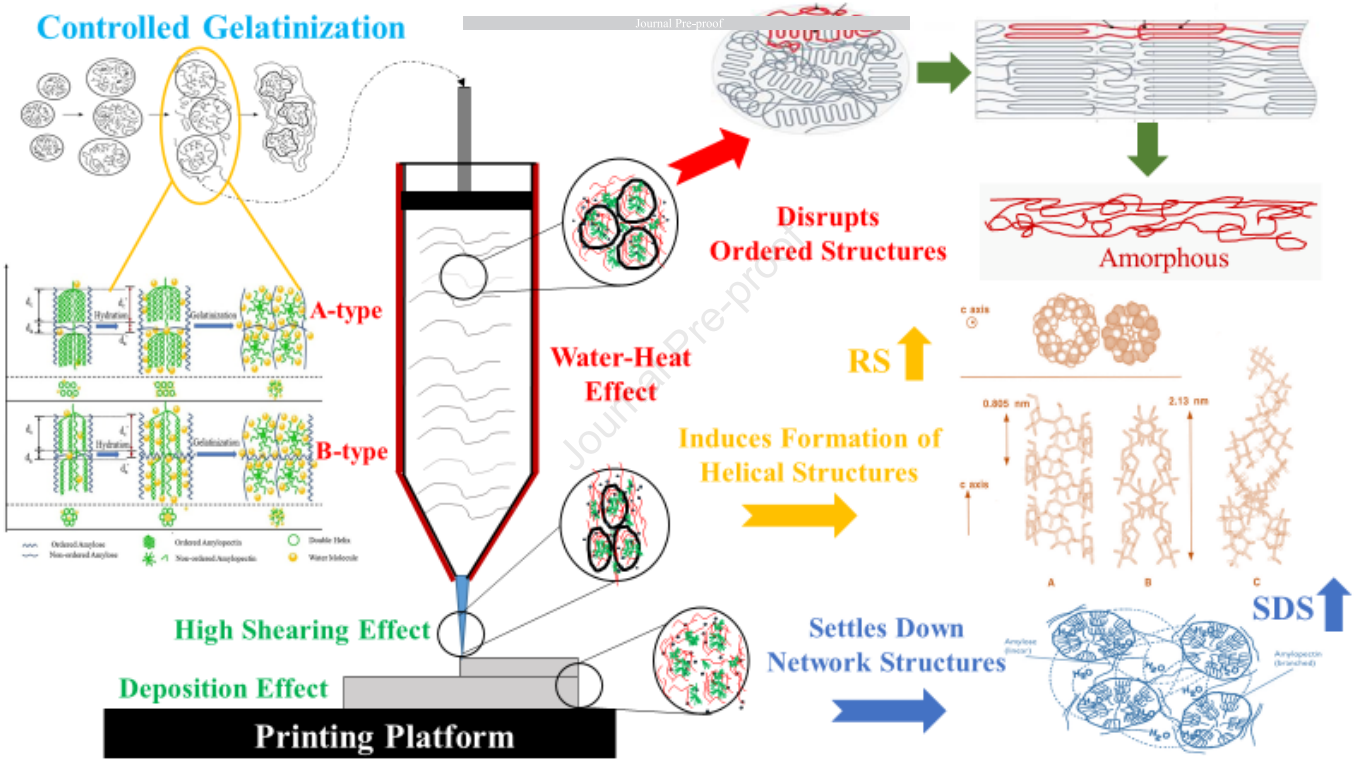

Effect of pre-printing gelatinization degree on the structure and digestibility of hot-extrusion 3D-printed starch

Bo Zheng [a], Yukuo Tang [a], Fengwei Xie [b]**, Ling Chen [a]*

[a] School of Food Science and Engineering, Guangdong Province Key Laboratory for Green Processing of Natural Products and Product Safety, Engineering Research Center of Starch and Vegetable Protein Processing Ministry of Education, South China University of Technology, Guangzhou 510640, China

[b] International Institute for Nanocomposites Manufacturing (IINM), WMG, University of Warwick, Coventry, CV4 7AL, United Kingdom

*Corresponding author. E-mail: felchen@scut.edu.cn (L. Chen)

**Corresponding author. Email: d.xie.2@warwick.ac.uk. fwhsieh@gmail.com (F. Xie)

ABSTRACT: Hot-extrusion 3D printing (HE-3DP) is an emerging technique to create customized food with desired structure and properties. This research is focused on the effect of pre-printing gelatinization degree on the structure and digestibility of rice and wheat starch gels after HE-3DP. The results show that the lamellar, crystalline and helical structures were destroyed, the compactness of nano-aggregates formed decreased significantly, the content of semi-bound water in the gel system increased, and the content of bound water decreased, and these changes were more significant with an increasing gelatinization degree. Interestingly, the ideal printability and digestion resistance of the printed materials could be obtained with the pre-printing gelatinization degrees of rice and wheat starches being 50% and 40%, respectively. Overall, the pre-printing gelatinization degree has been found to be an important factor in regulating the printability and digestibility of starch during HE-3DP.

Keywords: Hot-extrusion 3D printing; starch; gelatinization degree; digestibility; ordered structure

Abbreviations

HE-3DP	Hot-extrusion 3D printing
RG	Rice starch gel
WG	Wheat starch gel
RDS	Rapidly digestible starch
SDS	Slowly digestible starch
RS	Resistant starch
RC	Relative crystallinity

1 Introduction

With starch-based food playing an important role in the human diet, the nutritional function of starch has attracted great attention. Many studies have shown that the nutritional attributes of starch are determined by its digestibility in the human body (J. Guo, Tan, & Kong, 2020; Zheng, et al., 2018). Based on the rate and extent of the digestion in vitro, starch is classified as rapidly digestible starch (RDS), slowly digestible starch (SDS), and resistant starch (RS) (Magallanes‐Cruz, Flores‐Silva, & Bello‐Perez, 2017; Zheng, Zhong, Tang, & Chen, 2020). Among them, foods with a high RDS content will cause rapid and dramatic changes in the postprandial insulin level, accompanied by a rapid glycemic response initially and a higher free fatty acid content in the longer term, which may lead to the risk of metabolic complications such as diabetes and hypertension (Ells, Seal, Kettlitz, Bal, & Mathers, 2005). However, the consumption of foods with high contents of SDS and RS can alleviate or eliminate the adverse effects of RDS on human health. SDS can reduce the glycemic response and help to prevent and control diseases caused by hyperglycemia (Giuberti & Gallo, 2018). RS is fermented by microorganisms as a dietary fiber in the colon, which can prevent intestinal diseases and maintain colon health (Hendrich, Birt, Li, & Zhao, 2013; Kendall, Azadeh, Augustin, & Jenkins, 2004). Therefore, increasing the contents of SDS and RS in starch can effectively improve its nutritional functions.

The digestibility of starch is determined by its structure (H. Wang, et al., 2018). In particular, the changes in the crystalline and amorphous structures of starch materials are a comprehensive manifestation of the variations of the chain structure and the way of stacking,

influencing the digestibility of the starch materials (Poulhazan, Arnold, Warschawski, & Marcotte, 2018; Suntharamoorthy, 2017). However, reported studies on the relationship between multi-scale structure and digestibility mainly focused on the structural changes on a certain scale, without considering the overall structure from the perspective of structural domains, and also rarely paid attention to the effect of amorphous structure on the digestibility of starch. It is generally believed that rapid digestion of starch results from the amorphous structure, while the performance of slow digestion and digestion resistance is positively correlated with the crystalline structure (Rodriguez-Garcia, et al., 2020). Zhang et al. reported that the A-type crystalline structure with a large number of short chains and branches in grain starch determines the influencing factors for its SDS content (Zhang, Ao, & Hamaker, 2006). Using ^{13}C NMR spectroscopy to study tapioca starch isolated by enzymes, Mutungi et al. found that the crystalline structure is the main structure that determines the RS content in starch (Mutungi, et al., 2011). Therefore, the effects of crystalline and amorphous domains of starch materials on their digestibility can be understood by regulating starch structures through processing. Besides, the relationship between starch structures and digestibility is worth further clarification.

Hot-extrusion 3D printing (HE-3DP) technology has the advantage of being able to personalize the appearance and customize the nutrition in the food field. However, the research on the HE-3DP of starchy materials is still in its infancy. Normally, starch needs to be pre-gelatinized and made into a gel before HE-3DP. The gel will be subjected to heat and shear treatment in the heating cylinder, which modifies its structure and adjusts its rheological

properties and printability (Theagarajan, Moses, & Anandharamakrishnan, 2020). Our group previously investigated the effects of starch concentration on HE-3DP printability for different starches (Chen, Xie, Chen, & Zheng, 2019; Z. P. Liu, Chen, Zheng, Xie, & Chen, 2020) and established the relationship between structure, rheological properties and 3D printability for starch gels, which provided an insight into predicting the rheological properties and printability of starch materials and selecting suitable printing conditions to regulate starch structures for suitable rheological properties (Zeng, Chen, Chen, & Zheng, 2021). Hitherto, there has been no study concerning the use of 3D printing to regulate the digestibility of starch. However, modifying starch structures, especially crystalline and amorphous domains, by 3D printing to regulate starch digestibility will provide new ideas for the creation of healthy foods.

In this paper, according to the structural characteristics of SDS and RS and the results of previous research on printability, the effect of pre-printing gelatinization degree on the structures and in vitro digestibility of starch materials produced by HE-3DP was investigated. More specifically, the changes in printability and digestibility were correlated to the structural changes in crystalline and amorphous domains and the unwinding/winding behavior of starch chains. The understanding from this work can be instrumental to the rational design of HE-3DP processes for producing starch products with greater anti-digestion properties.

2 Materials and methods

2.1 Main experimental materials

Food-grade rice starch (>99% purity, 14.26% moisture content) and wheat starch (>99% purity, 14.38% moisture content) were purchased from Jiangxi Jinnong Biotechnology Co., Ltd.

and Anhui Ante Food Co., Ltd. (China), respectively. Sodium hydroxide, absolute ethanol, trihydrate sodium acetate, and acetic acid, all analytically pure, were supplied by Tianjin Baishi Chemical Co., Ltd., Tianjin Chemical Reagent Factory, Jiangsu Qiangsheng Functional Chemical Co., Ltd., and Tianjin Hongda Chemical Reagent Factory (China), respectively. Pancreatic α-amylase and amyloglucosidase were obtained from Sigma Company (USA). A glucose oxidation kit was purchased from Megazyme Company (Ireland).

2.2 Sample preparation

Starch samples with different gelatinization degrees were prepared following the previous studies with slight modification (Chen, et al., 2019; Parada & Aguilera, 2009). Rice starch and wheat starch were heated for 60 min at a constant temperature selected between 54 and 74 °C and then cooled to 10 °C to obtain samples with different gelatinization degrees. Then, the thermal properties of starch samples were determined using a differential scanning calorimeter (8000, Perkin Elmer, USA). An empty aluminum pan was used as the reference. Starch samples (4 mg, dry mass) were weighed accurately into aluminum pans and 13 mg of deionized water was added. The pans were sealed and equilibrated at 4 °C overnight before analysis. Meanwhile, the samples were scanned against a blank (empty pan) from 30 to 100 °C at a rate of 10 °C/min. The gelatinization degree of starch samples was calculated against that of native rice and wheat starch according to Eq.(1):

$$Gelatinization\ \ degree\ \ (\%) = \left(1 - \frac{\Delta H_{Sample}}{\Delta H_{Native}}\right) \times 100 \qquad (1)$$

where ΔH_{sample} is the enthalpy change of the treated starch sample and ΔH_{native} is the enthalpy change of native starch. Numerical results are averages of three replicates.

From DSC results and **Eq. (1)**, the gelatinization *vs.* temperature curves (**Figure S1**) and fitting functions (**Table S1**) for rice starch and wheat starch were established. Rice starch and wheat starch pastes with gelatinization degrees of 30%, 40%, 50%, 60%, and 70% and a concentration of 15% (w/w) were obtained. Then, these starch pastes were immediately placed in the printer cartridge for printing according to a preset program. HE-3DP was performed on a SHINNOVE-S2 printer (Shiyin, China) according to our reported method (Z. P. Liu, et al., 2020). Firstly, the prepared suspension was transferred to the printing cylinder and equilibrated at 60 °C for 5 min. Then, printing was carried out and the main printing parameters included a nozzle diameter of 0.8 mm and a nozzle speed of 30 mm/s. After printing, the obtained samples were frozen overnight at −80 °C in an ultra-low temperature refrigerator, then lyophilized in a vacuum freeze dryer, crushed through a 60-mesh sieve, and measured for the moisture content of the samples before starch digestibility test. The rice starch samples with pre-printing gelatinization degrees of 30–70% were denoted as RG-30, RG-40, RG-50, RG-60, and RG-70, respectively, and the wheat starch samples with pre-printing gelatinization degrees of 30–70% were denoted as WG-30, WG40, WG-50, WG-60, and WG-70, respectively.

2.4 Characterization

Small-angle X-ray scattering analysis (SAXS) was performed on a SAXS system (Anton Paar, Graz, Austria) following our previous study (Zeng, et al., 2021). The obtained data were normalized and processed using the SAXS Quant 3.0 software.

X-ray diffraction (XRD) analysis was measured using a powder X-ray diffractometer (PANalytical Co., Almelo, Netherlands) following our previous study (Zheng, Wang, Wang,

Chen, & Zhou, 2020). MDI Jade software (Version 6.0) was used to calculate relative crystallinity (*RC*) following our previous study (Zheng, Wang, et al., 2020).

Solid-state cross-polarization magic angle spinning carbon-13 nuclear magnetic resonance (CP/MAS ^{13}C NMR) analysis was performed on a Bruker AVANCE III HD 400 spectrometer (Bruker, Germany) equipped with a 4-mm broadband double-resonance MAS probe following our previous study (K. Liu, Zhang, Chen, Li, & Zheng, 2019).

Low-field nuclear magnetic resonance (LF-NMR) analysis was performed using a 23 MHz NMR analyzer (NMI20-040H-I, Niumag Analytical Instrument Co., Ltd., Suzhou, China). Approximately 3 g of the pasting sample was transferred to a 10 mm diameter NMR glass tube and sealed with Parafilm to prevent evaporation during the experiments. The spin-spin relaxation time (T2) measurements were performed using the Carr-Purcell-Meiboom-Gill (CPMG) sequence. The experimental parameters used are as follows: the number of echoes for the CPMG sequence was 1024, the number of scans was 8, and the time domain spin-echo decay ranged between 1000 and 2000 ms. Data fitting was performed by using the instrument software (M. Tang, Yan, Gu, Zhang, & Cai, 2013).

In vitro digestibility was determined by a modified Englyst method as used in our previous studies (T. Guo, Hou, Liu, Chen, & Zheng, 2021; K. Liu, et al., 2019). Porcine pancreatic enzymes (3 g) were homogeneously mixed with 20 mL of deionized water, and the mixture was centrifuged at 3000 g for 15 min to obtain the supernatant. Then, 13.5 mL of the supernatant was mixed with 225 U of amyloglucosidase and 1 mL of deionized water to prepare the enzyme solution. Starch (1.0 g, dry starch base) was dispersed in 20 mL of acetate buffer solution (0.1

M, pH = 5.2). Samples were equilibrated at 37 °C, and 5 mL of the fresh enzyme solution containing pancreatin and amyloglucosidase was added respectively. Thereafter, starch was incubated at 37 °C with continuous shaking (190 rpm), and 0.5 mL aliquots of hydrolyzed solution were withdrawn at preset time intervals (20 and 120 min) and mixed with 20 mL of 70% ethanol (w/w) immediately. A centrifuge was used at a speed of 3000 g for 5 min to collect the supernatant, and the glucose content released during digestion was measured by the GOPOD method. Each sample was analyzed in triplicate.

The data obtained through at least triplicate experiments were analyzed using SPSS software (Version 23.0), and related data were presented as average ± standard deviation (SD). The significant difference test was performed using analysis of variance (ANOVA) and Duncan's test. The difference was deemed to be significant in statistics with $p < 0.05$.

3 Results and discussion

3.1 Printability

Figure 1 shows the morphology of the printed rice and wheat starch samples with gelatinization degrees of 30–70%. In general, the printed rice starch with gelatinization degrees of 30–40% showed poor morphological integrity and insufficient resolution. In contrast, with the degree of gelatinization increased to 50%, a clear morphology, smooth surface, and high resolution could be achieved. However, as the degree of gelatinization further increased to 60–70%, there were more depressions in the sample, indicating that an increased breakage rate of the printed filaments. The printed wheat starch samples showed the same trend as rice starch.

3.2 Nano-aggregated structure

Figure 2A shows the SAXS double-logarithmic graphs of the printed starch samples. For the printed rice and wheat starch samples with different gelatinization degrees, the SAXS scattering peak at q = 0.6–0.7 nm^{-1} disappeared, indicating that the original lamellar structure of the native starches was destroyed by the combinational action of water, heat, and shear during the HE-3DP process. By performing power-law fitting (I *vs.* $q^{-\alpha}$) on the linear region in the low q range, the information about the fractal dimension of aggregates could be obtained and the associated data are shown in Table 1. The α values of the printed rice and wheat starch samples were in the range of 1–3, indicating these starch materials changed from a surface fractal structure into a mass fractal structure through printing. Besides, the aggregated structure in the materials became loose. When the degree of gelatinization increased, the value of α gradually decreased ($p < 0.05$), indicating that HE-3DP caused the starch materials to form a looser structure dominated by amorphous domains, and the degree of gelatinization would affect the compactness of nano-aggregates arranged. In addition, when the pre-printing gelatinization degree increased from 50% to 60%, the α value of the printed rice starch sample decreased significantly, showing that the arrangement of nano-aggregates became looser. The printed wheat starch sample showed the same trend when the degree of gelatinization before printing increased from 40% to 50%.

To further understand the submicroscopic structure of the 3D-printed starch samples, Kratky plots fitting models (q^2*$I(q)$ *vs.* q) were used (**Figure 2B**) according to the Lorentz equation and the related data were also shown in **Table 1**. The peak in Kratky plots at low q

206 indicated the presence of inhomogeneity in the gel network system (Kobayashi, et al., 1994).
207 In our previous studies, corn starch and potato starch gels showed no distinctive peaks at low q
208 while rice starch showed a weak scattering peak at a q value of 0.4 nm^{-1} in Kratky plots,
209 indicating the existence of structural inhomogeneity on a submicroscopic level. In this study,
210 we found that with an increasing pre-printing gelatinization degree, the intensity of the Kratky
211 scattering curve peak for both starches decreased (Z. P. Liu, et al., 2020; Zeng, et al., 2021).
212 These results further demonstrated the existence of structural inhomogeneity in the starch
213 materials after HE-3DP, which indicates locally ordered structures in the amorphous domains.
214 Moreover, this heterogeneity could decrease with an increasing pre-printing gelatinization
215 degree. Regarding this, during printing, starch gel materials were subjected to water, heat, and
216 mechanical forces in the barrel, which promoted starch chains to be in a dynamic equilibrium
217 of disordering and re-ordering. In particular, the starch gel material underwent a sudden change
218 from a high-shear condition to a shear-free condition while being extruded out of the nozzle.
219 Shearing could facilitate chain orientation and rearrangement. Furthermore, the deposition
220 process on the printing platform would allow the rearrangement and aggregation of starch
221 chains, thereby forming a new partially ordered structure.

222 DB-P equations were used to fit SAXS curves for quantitatively analyzing the
223 submicroscopic structure of the starch gels, and the characteristic lengths of the non-uniform
224 system in the printed rice and wheat starch samples with different pre-printing gelatinization
225 degrees are shown in **Table 1**. It could be seen that the characteristic length Ξ for the two types
226 of starch gel materials increased first and then decreased with an increasing gelatinization

227 degree ($p < 0.05$), suggesting the structural inhomogeneity on a submicroscopic level also first
228 increased and then decreased with a higher pre-printing gelatinization degree. For the rice starch
229 samples with pre-printing gelatinization degrees of 30–50% and the wheat starch samples with
230 pre-printing gelatinization degrees of 30–40%, there were some ordered structure domains such
231 as ungelatinized granules and crystallites in the system. As a result, the homogeneity of the
232 submicroscopic structure in the printed starches increased. Compared with that of the printed
233 wheat starch samples, the submicroscopic structure in the printed rice starch sample showed a
234 greater degree of inhomogeneity.

235 ## 3.3 Crystalline structure

236 **Figure 2C** shows the XRD curves of the printed starch samples with different pre-printing
237 gelatinization degrees. All the samples showed diffraction peaks at 12.9° and 20.2° (2θ), while
238 the original characteristic peak of the A-type crystalline structure was absent. This result shows
239 that the HE-3DP process could predominantly destroy the original crystalline structure which
240 was contributed by stacked double helices and single helices but result in the formation of a
241 new V-type crystalline structure due to the re-arrangement of starch chains (B., C., M., & A.,
242 2017). **Table 1** shows that for both the printed rice and wheat starches, the relative crystallinity
243 decreased as the pre-printing gelatinization degree increased.

244 ## 3.4 Helical structure

245 The relative content of the double helices formed by amylopectin side chains and the V-
246 type single helices formed by amylose in starch materials can be calculated from the ^{13}C NMR
247 spectra (Tan, Flanagan, Halley, Whittaker, & Gidley, 2007). The helical structure results for the

printed wheat and rice starch samples were shown in **Figure 2D** and **Table 1**. As the degree of gelatinization of starch before printing increased, the content of double helices in the two types of starch materials decreased significantly ($p < 0.05$), while the content of the single-helical structure firstly increased and then decreased. In this regard, for starch with a low pre-printing gelatinization degree, the hydrothermal and shear effects during HE-3DP could further destroy double helices and lead to the formation of single helices. When the sample for printing was already highly gelatinized, it is highly disordered and there would be a high degree of chain mobility. In this case, residual double helices would be further destroyed during HE-3DP and there was a low tendency to form single helices. With an increasing pre-printing gelatinization degree, HE-3DP resulted in a less reduction in the content of double helices and a less increase in the content of single helices for wheat starch samples than for rice starch. Accordingly, the printed wheat starch had a higher degree of submicroscopic structure inhomogeneity, as discussed above.

3.5 Low-field NMR analysis

The content, distribution and fluidity of water, the way of action of starch molecules, or the transformation of starch molecules from micelles into a network structure will have a significant impact on the microstructure and macroscopic properties of starch gel materials (S. Wang, Li, Zhang, Copeland, & Wang, 2016). LF-NMR can detect the spin-lattice (T_1) relaxation and spin-spin (T_2) relaxation time constants caused by different chain mobility in the system (Pitombo & Lima, 2003). The T_2 relaxation time of starch gel materials can usually be divided into 2–3 proton peaks. The first proton peak represents the interaction between protons in the

crystal lattice, that is, the proton interaction in the crystalline structure of starch materials. The second and third proton peaks are produced by protons in a more mobile environment, which indicates the interaction between water protons and —OH protons on starch chains (H.-R. Tang, Brun, & Hills, 2001; Washburn & Birdwell, 2013). The position and size of these relaxation peaks are affected by both the state of the sample and the ambient temperature (Ezeanaka, Nsor-Atindana, & Zhang, 2019). Therefore, a smaller T_2 relaxation time usually means strong interaction between water and starch (Antje, Gonera, Paul, & Cornillon, 2002; Lechert, 1981; Siqi Wang, Lin, & Tan, 2020).

Figure 2 and **Table 2** show the T_2 relaxation time parameters of the printed starch samples with different pre-printing gelatinization degrees. The starch gel materials after HE-3DP only showed two proton peaks (T_{21} and T_{22}) on the LF-NMR curve, which correspond to the proton peak positions of "bound water" and "semi-bound water", respectively. Increasing the pre-printing gelatinization degree reduced the relaxation time and the peak area ratio of the T_{21} proton peak, suggesting the proportion of bound water in the printed starches decreased but there was strong interaction between starch and water. This also indicates that the ordered structure in the starch materials was not completely destroyed, and in the printed sample, the ordered structure was the part of the material that was more closely bound to water molecules, which is consistent with the results of SAXS, XRD and ^{13}C NMR. Besides, the relaxation time of the T_{22} proton peak and the peak area ratio also increased significantly with an increasing pre-printing gelatinization degree, indicating the network structure in the amorphous domains

was more uniform, the ability of starch to bind water molecules was weakened, and the content of semi-bound water, which had weaker interaction with starch chains, was increased.

In addition, it can also be seen from **Table 2** that the ratio of T_{21} in the printed rice starch was higher than that of the printed wheat starch, suggesting that there was a higher content of bound water in the printed rice starch samples. This result might be related to the higher crystallinity of the printed rice starch materials. In contrast, the content of semi-bound water in the printed wheat starch materials was higher, which may be correlated with the proportion of amorphous content in the material.

3.6 *In vitro* digestibility

Table 2 showed the digestibility of the printed starch samples with different pre-printing gelatinization degrees. RG-100 and WG-100 were the printed samples that were completely gelatinized. The SDS, SDS and RS contents of RG-100 were 92.47%, 5.64%, and 1.89%, respectively while those of WG-100 were 93.83%, 4.65%, and 1.52%, respectively. Compared with those of the printed completely gelatinized sample, the RDS contents of the samples with pre-printing gelatinization degree of 30–70% after printing were somehow lower, while their SDS and RS contents were significantly higher. In general, SDS is contributed by amorphous domains containing regularly arranged chains and crystalline domains with some imperfection, while the structural basis of RS is perfectly arranged crystallites (Chi, et al., 2021; He, Zheng, Wang, Li, & Chen, 2020). Therefore, the results indicate that printed starch samples still retain some crystallites or short-range ordered structures. As the gelatinization degree increased, the RDS content in the printed samples increased significantly, accompanied by significant

decreases in the SDS and RS contents. The SDS and RS contents of the printed rice starch were decreased from 18.41% to 5.64% and from 15.09% to 1.89%, respectively. Similarly, the SDS and RS contents of the printed wheat starch were decreased from 20.45% to 4.65% and from 10.72% to 1.52%. Studies (Ashogbon & Akintayo, 2014; Ratnayake & Jackson, 2007) have shown that gelatinization can destroy ordered starch structures, which are the structural basis of SDS and RS. In this way, it is expected to see the digestion resistance decreases with a higher degree of gelatinization before printing in this work. For the two types of starch materials with the same pre-printing gelatinization degree, the RDS content of the printed wheat starch samples was higher than those of the printed rice starch. Though both the printed rice and wheat starches had the A-type crystalline structure, the printed rice starch samples had higher crystallinity and more short-range ordered structure as reflected by their higher α value and contents of double and single helices, resulting in higher SDS and RS contents.

Overall, according to the print topography and digestion data, the degree of gelatinization would significantly affect the printability and digestibility of the printed starch gels. Interestingly, the samples with better printability have higher SDS and RS contents, while the samples with broken filaments or a collapsed printed structure had a significantly higher RDS content, suggesting that the printed starch gels had consistency between printability and digestibility. The desired structure of starch gel could be obtained by optimizing the printing conditions, thus realizing the regulation of printing formability and digestion performance. The results showed that for rice and wheat starches for HE-3DP, ideal printing formability and

reduced digestibility could be achieved with pre-printing gelatinization degrees being 50% and 40%, respectively.

3.7 Structural contributions to digestibility

Based on the above discussion on the differences in structures, printability, and digestibility among different starch samples subjected HE-3DP, a schematic representation of how pre-printing gelatinization degree regulates the structural domain and digestion performance of printed starch gels is proposed and shown in **Figure 4**. When starch enters the hot-extrusion 3D-printer barrel, it experiences the destruction of original hydrogen bonds between starch chains with the migration of water molecules, and is subjected to heat which promotes the migration of water molecules and increases starch chain mobility. Both effects could promote the depolymerization of starch molecular chains, the unwinding of double helices, the destruction of crystalline and lamellar structures, and the swelling and fragmentation of starch granules, resulting in further transformation of ordered starch structures into a disordered state. When starch gel is extruded out of the confined space of the nozzle, it underwent a sudden change from a high-shear condition to a shear-free situation. Shearing can promote the orientation and rearrangement of disordered starch chains and deposition may also allow the rearrangement and aggregation of disordered starch chains, leading to new short-range ordered structures (e.g. helices), nano-aggregates, and crystalline structure. These may contribute to a dense structure that could hinder the attack by amylase on glycosidic bonds, thereby reducing the digestibility of starch.

The improvement in the anti-digestion properties of starch materials depended on the degree of retention of ordered structures in the crystalline and amorphous domains as well as the formation of new ordered structures during HE-3DP. Previous studies showed that with a higher gelatinization degree of the pre-printing starch sample, the ordered structures including crystallites and helices in the starch material have been mostly destroyed and transformed into a looser amorphous structure, with greater chain mobility (Hari, Garg, & Garg, 1989; Parada & Aguilera, 2012). This makes it easier for HE-3DP to further destroy starch structures but more difficult for starch chains to reassemble into ordered structures, ultimately resulting in lower digestion resistance. On the other hand, starch with a low degree of gelatinization contains some ungelatinized starch granules and a high content of ordered structures. In this case, ordered starch structures are less easy to be destroyed during printing as the mobility of water molecules could be lower and the heat conduction and shearing could be less efficient. But in this case, disordered starch chains are more likely to re-aggregate to form a new locally ordered structure, which promotes the generation of SDS and RS during extrusion and deposition and leads to printed starch materials with lower digestibility. Due to the more ordered structure formed during HE-3DP, the SDS and RS contents of rice starch were higher than that of wheat starch. Moreover, it could be seen that the changes in the crystalline structure, amorphous structure, and microphase structure uniformity of starch gel caused by different gelatinization degrees led to different rheological properties, thereby resulting in different printability.

4 Conclusion

In this paper, the relationship between structure (crystalline and amorphous domains and microphase structure uniformity), printability, and digestibility for rice and wheat starches with different pre-printing gelatinization degrees were explored. For starch gels with a low pre-printing gelatinization degree, due to the existence of granule structure and ordered structures (e.g. crystallites and helices), it is easier to promote the aggregation of molecular chains and the formation of new ordered structures during HE-3DP. For starch gel materials with a higher gelatinization degree, the structure was mainly amorphous and loose, and the starch chains had higher mobility. In this case, HE-3DP is more likely to further disrupt starch structures and it is more difficult for the starch chains to rearrange into ordered structures. Interestingly, the ideal printability and digestibility could be obtained when their gelatinization degrees of rice starch and wheat starch were 50% and 40%, respectively. Overall, this study could provide useful information for the design of healthy starch-based foods by HE-3DP.

5 Declaration of Interest

The authors declare to have no conflict of interests.

6 Acknowledgements

This work was supported by the National Natural Science Foundation of China (31871751), the Key Project of the Guangzhou Science and Technology Program (201804020036), and the China Postdoctoral Science Foundation (2021M691069).

References

Antje, Gonera, Paul, & Cornillon. (2002). Gelatinization of Starch/Gum/Sugar Systems Studied by using DSC, NMR, and CSLM. *Starch □ Stärke, 54*(11), 508-516.

Ashogbon, A. O., & Akintayo, E. T. (2014). Recent trend in the physical and chemical modification of starches from different botanical sources: A review. *Starch□Stärke, 66*(1-2), 41-57.

B., G., C., P. S., M., S., & A., D. J. (2017). Development of an infusion method for encapsulating ascorbyl palmitate in V-type granular cold-water swelling starch. *Carbohydrate Polymers Scientific & Technological Aspects of Industrially Important Polysaccharides*.

Chen, H., Xie, F. W., Chen, L., & Zheng, B. (2019). Effect of rheological properties of potato, rice and corn starches on their hot-extrusion 3D printing behaviors. *Journal of Food Engineering, 244*, 150-158.

Chi, C., Li, X., Huang, S., Chen, L., Zhang, Y., Li, L., & Miao, S. (2021). Basic principles in starch multi-scale structuration to mitigate digestibility: A review. *Trends in Food Science & Technology*.

Ells, L. J., Seal, C. J., Kettlitz, B., Bal, W., & Mathers, J. C. (2005). Postprandial glycaemic, lipaemic and haemostatic responses to ingestion of rapidly and slowly digested starches in healthy young women. *British Journal of Nutrition, 94*(6), 948-955.

Ezeanaka, M. C., Nsor-Atindana, J., & Zhang, M. (2019). Online low-field nuclear magnetic resonance (LF-NMR) and magnetic resonance imaging (MRI) for food quality optimization in food processing. *Food and Bioprocess Technology, 12*(9), 1435-1451.

Giuberti, G., & Gallo, A. (2018). Reducing the glycaemic index and increasing the slowly digestible starch content in gluten□free cereal□based foods: A review. *International Journal of Food Science & Technology, 53*(1), 50-60.

Guo, J., Tan, L., & Kong, L. (2020). Impact of dietary intake of resistant starch on obesity and associated metabolic profiles in human: a systematic review of the literature. *Critical reviews in food science and nutrition*, 1-17.

Guo, T., Hou, H., Liu, Y., Chen, L., & Zheng, B. (2021). In vitro digestibility and structural control of rice starch-unsaturated fatty acid complexes by high-pressure homogenization. *Carbohydrate Polymers, 256*, 117607.

Hari, P. K., Garg, S., & Garg, S. K. (1989). Gelatinization of Starch and Modified Starch. *Starch □ Strke, 41*(3), 88-91.

He, H., Zheng, B., Wang, H., Li, X., & Chen, L. (2020). Insights into the multi-scale structure and in vitro digestibility changes of rice starch-oleic acid/linoleic acid complex induced by heat-moisture treatment. *Food Research International, 137*, 109612.

Hendrich, S., Birt, D. F., Li, L., & Zhao, Y. (2013). *Colon Health and Resistant Starch: Human Studies and Animal Models*: Resistant Starch: Sources, Applications and Health Benefits.

Kendall, C., Azadeh, E., Augustin, L., & Jenkins, D. (2004). Resistant starches and health. *Journal of Aoac International, 87*(3), 769-774.

Kobayashi, M., Yoshioka, T., Kozasa, T., Tashiro, K., Suzuki, J., Funahashi, S., & Izumi, Y. (1994). Structure of Physical Gels Formed in Syndiotactic Polystyrene/Solvent Systems Studied by Small-Angle Neutron Scattering. *Macromolecules, 27*(6), 1349-1354.

Lechert, H. T. (1981). *Water Binding On Starch: NMR Studies On Native And Gelatinized Starch*.

Liu, K., Zhang, B., Chen, L., Li, X., & Zheng, B. (2019). Hierarchical structure and physicochemical properties of highland barley starch following heat moisture treatment. *Food Chemistry, 271*, 102-108.

Liu, Z. P., Chen, H., Zheng, B., Xie, F. W., & Chen, L. (2020). Understanding the structure and rheological properties of potato starch induced by hot-extrusion 3D printing. *Food Hydrocolloids, 105*, 105812.

Magallanes□Cruz, P. A., Flores□Silva, P. C., & Bello□Perez, L. A. (2017). Starch structure influences its digestibility: a review. *Journal of Food Science, 82*(9), 2016-2023.

Mutungi, C., Onyango, C., Doert, T., Paasch, S., Thiele, S., Machill, S., Jaros, D., & Rohm, H. (2011). Long- and short-range structural changes of recrystallised cassava starch subjected to in vitro digestion. *Food Hydrocolloids, 25*(3), 477-485.

Parada, J., & Aguilera, J. M. (2009). In vitro Digestibility and Glycemic Response of Potato Starch is Related to Granule Size and Degree of Gelatinization. *Journal of Food Science, 74*(1), E34-E38.

Parada, J., & Aguilera, J. M. (2012). Effect of native crystalline structure of isolated potato starch on gelatinization behavior and consequently on glycemic response. *Food Research International, 45*(1), 238-243.

Pitombo, R. N., & Lima, G. A. (2003). Nuclear magnetic resonance and water activity in measuring the water mobility in Pintado (Pseudoplatystoma corruscans) fish. *Journal of Food Engineering, 58*(1), 59-66.

Poulhazan, A., Arnold, A. A., Warschawski, D. E., & Marcotte, I. (2018). Unambiguous ex situ and in cell 2D 13C solid-state NMR characterization of starch and its constituents. *International journal of molecular sciences, 19*(12), 3817.

Ratnayake, W. S., & Jackson, D. S. (2007). A new insight into the gelatinization process of native starches. *Carbohydrate Polymers, 67*(4), 511-529.

Rodriguez-Garcia, M. E., Hernandez-Landaverde, M. A., Delgado, J. M., Ramirez-Gutierrez, C. F., Ramirez-Cardona, M., Millan-Malo, B. M., & Londoño-Restrepo, S. M. (2020). Crystalline Structures of the main components of Starch. *Current Opinion in Food Science*.

Suntharamoorthy, M. (2017). *Factors influencing starch chain realignment and interactions within the amorphous and crystalline domains of pulse and high amylose maize starches on annealing.* Memorial University of Newfoundland.

Tan, I., Flanagan, B. M., Halley, P. J., Whittaker, A. K., & Gidley, M. J. (2007). A method for estimating the nature and relative proportions of amorphous, single, and double-helical components in starch granules by 13C CP/MAS NMR. *Biomacromolecules, 8*(3), 885-891.

Tang, H.-R., Brun, A., & Hills, B. (2001). A proton NMR relaxation study of the gelatinisation and acid hydrolysis of native potato starch. *Carbohydrate Polymers, 46*(1), 7-18.

Tang, M., Yan, H., Gu, Z., Zhang, Y., & Cai, X. (2013). The effect of xanthan on short and long□term retrogradation of rice starch. *Starch □ Stärke, 65*(7□8).

Theagarajan, R., Moses, J. A., & Anandharamakrishnan, C. (2020). 3D Extrusion Printability of Rice Starch and Optimization of Process Variables. *Food and Bioprocess Technology, 13*(6), 1048-1062.

Wang, H., Liu, Y., Chen, L., Li, X., Wang, J., & Xie, F. (2018). Insights into the multi-scale structure and digestibility of heat-moisture treated rice starch. *Food Chemistry, 242*, 323-329.

Wang, S., Li, C., Zhang, X., Copeland, L., & Wang, S. (2016). Retrogradation enthalpy does not always reflect the retrogradation behavior of gelatinized starch. *Scientific Reports, 6*, 20965.

Wang, S., Lin, R., & Tan, M. (2020). Water dynamics changes and protein denaturation in surf clam evaluated by two-dimensional LF-NMR T1-T2 relaxation technique during heating process. *Food Chemistry, 320*, 126622.

Washburn, K. E., & Birdwell, J. E. (2013). A new laboratory approach to shale analysis using NMR relaxometry. In *Unconventional Resources Technology Conference* (pp. 1775-1782): Society of Exploration Geophysicists, American Association of Petroleum ….

Zeng, X., Chen, H., Chen, L., & Zheng, B. (2021). Insights into the relationship between structure and rheological properties of starch gels in hot-extrusion 3D printing. *Food Chemistry, 342*, 128362.

Zhang, G., Ao, Z., & Hamaker, B. R. (2006). Slow digestion property of native cereal starches. *Biomacromolecules, 7*(11), 3252.

Zheng, B., Wang, H., Shang, W., Xie, F., Li, X., Chen, L., & Zhou, Z. (2018). Understanding the digestibility and nutritional functions of rice starch subjected to heat-moisture treatment. *Journal of Functional Foods, 45*, 165-172.

Zheng, B., Wang, T., Wang, H., Chen, L., & Zhou, Z. (2020). Studies on nutritional intervention of rice starch-oleic acid complex (resistant starch type V) in rats fed by high-fat diet. *Carbohydrate Polymers, 246*, 116637.

Zheng, B., Zhong, S., Tang, Y., & Chen, L. (2020). Understanding the nutritional functions of thermally-processed whole grain highland barley in vitro and in vivo. *Food Chemistry, 310*, 125979.

Figure Captions

Fig. 1 Printed starch gel samples with different gelatinization degrees (RG, rice starch, WG, wheat starch; from left to right the gelatinization degrees are 30%, 40%, 50%, 60%, 70%, respectively)

Fig. 2 (A) SAXS double-logarithmic plots, (B) Kratky curves, (C) XRD patterns and (D) ^{13}C CP/MAS NMR spectra for the printed starch samples with different gelatinization degrees (RG, rice starch, WG, wheat starch; with gelatinization degrees of 30%, 40%, 50%, 60%, 70%, respectively)

Fig. 3 Transverse relaxation time spectra for the printed starch samples with different gelatinization degrees (RG, rice starch, WG, wheat starch; with gelatinization degrees of 30%, 40%, 50%, 60%, 70%, respectively)

Fig. 4 Schematic representation of the mechanism regarding the effect of the pre-printing gelatinization degree on the structure and digestibility of the starch after hot-extrusion 3D-printing

497 **Figures**

498

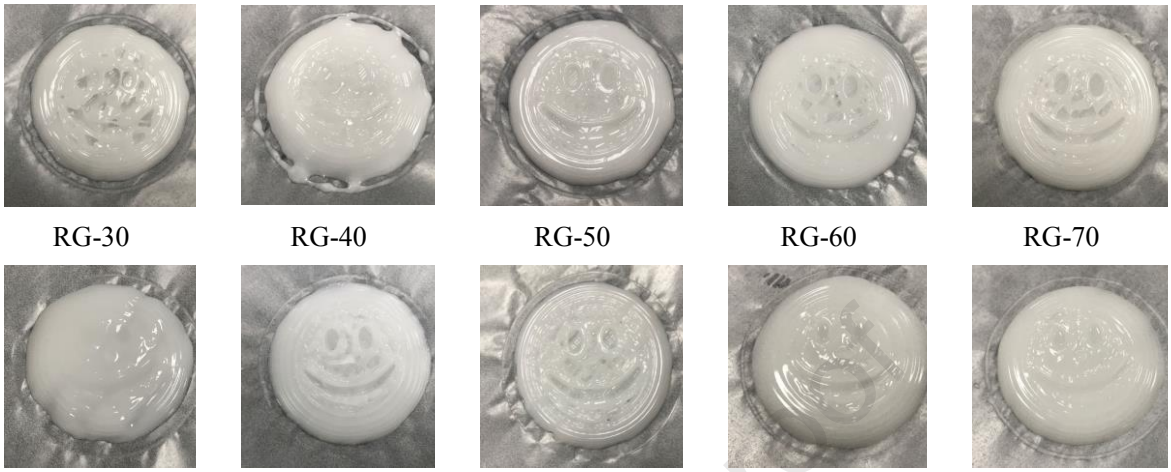

499

500 Figure 1

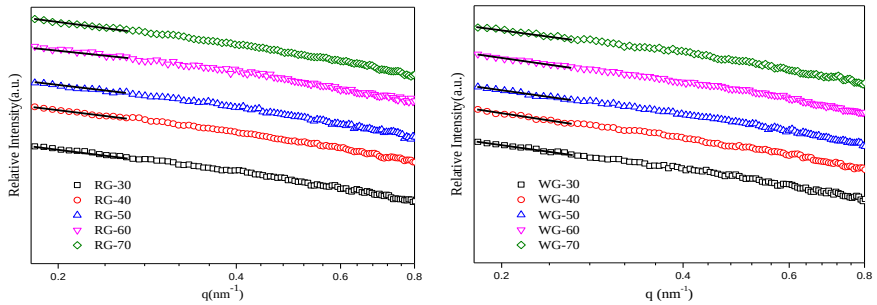

A

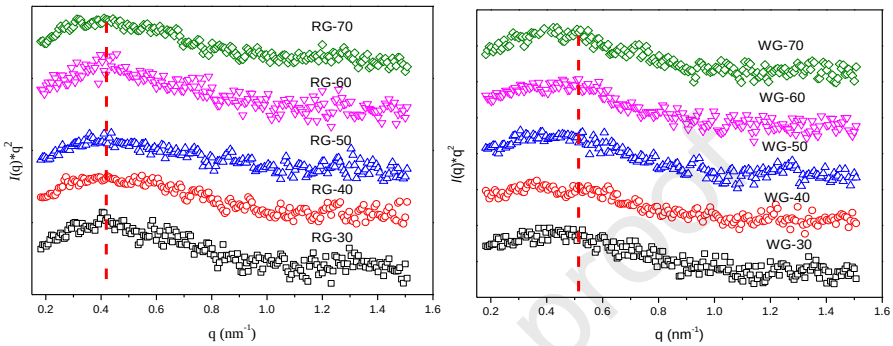

B

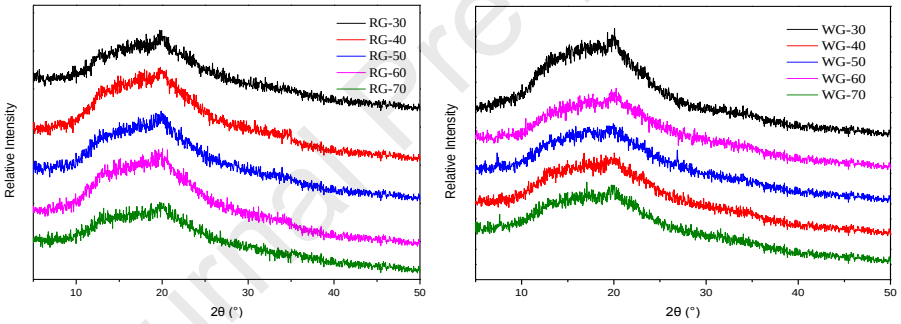

C

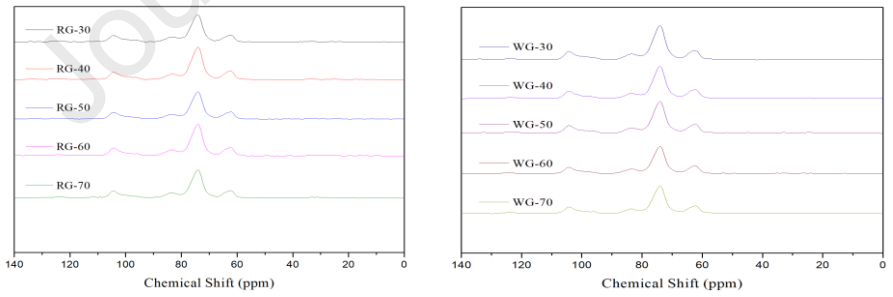

D

Figure 2

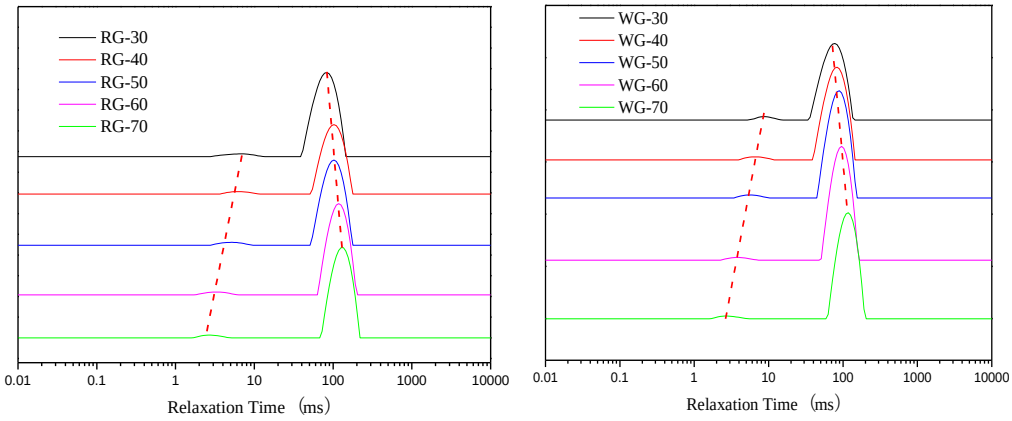

506

507 Figure 3

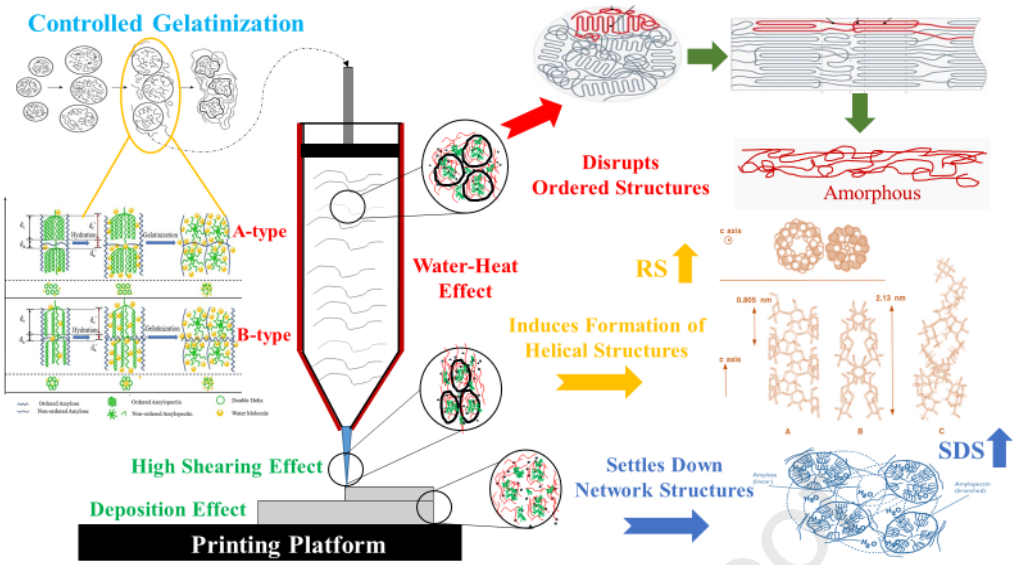

Figure 4

Tables

Table 1 SAXS parameters, RC and helical structure parameters of printed starch samples with different pre-printing gelatinization degrees

Samples	Ξ (nm)	R^2	α	D_m	RC (%)	Amorphous (%)	Double helix (%)	Single helix (%)
RG-30	3.25±0.07^{g}	0.999	1.96±0.07^{a}	1.96±0.07^{a}	22.31±0.52^{a}	63.60±0.33^{m}	29.26±0.30^{a}	7.14±0.78^{ef}
RG-40	3.47±0.03^{f}	0.999	1.92±0.03^{b}	1.92±0.03^{b}	19.84±0.25^{b}	67.94±0.55^{k}	22.36±0.71^{c}	9.70±0.61^{b}
RG-50	3.08±0.04^{h}	0.998	1.90±0.06^{b}	1.90±0.06^{b}	18.27±0.76^{c}	73.83±0.53^{i}	15.40±0.72^{f}	10.77±0.62^{a}
RG-60	2.81±0.06^{j}	0.997	1.74±0.05^{d}	1.74±0.05^{d}	17.55±0.88^{d}	79.51±0.70^{f}	13.63±0.67^{h}	6.86±0.65^{f}
RG-70	2.68±0.03^{l}	0.999	1.66±0.08^{e}	1.66±0.08^{e}	14.60±0.73f	85.30±0.69^{b}	9.39±0.37^{k}	5.31±0.48^{g}
WG-30	2.75±0.04^{k}	0.998	1.86±0.03^{c}	1.86±0.03^{c}	19.71±0.24^{b}	67.02±0.71^{l}	25.75±0.42^{b}	7.23±0.72^{e}
WG-40	2.83±0.06^{j}	0.998	1.82±0.06^{c}	1.82±0.06^{c}	17.83±0.40^{d}	72.10±0.71^{j}	18.34±0.67^{d}	9.56±0.38^{b}
WG-50	3.02±0.05^{h}	0.997	1.64±0.05^{e}	1.64±0.05^{e}	16.47±0.25^{e}	74.89±0.79^{h}	16.64±0.43^{e}	8.47±0.70^{c}
WG-60	2.93±0.08^{i}	0.997	1.57±0.08^{f}	1.57±0.08^{f}	13.82±0.51^{g}	77.38±0.30^{g}	14.73±0.44^{g}	7.89±0.34^{d}
WG-70	2.68±0.06^{l}	0.998	1.51±0.04^{g}	1.51±0.04^{g}	10.39±0.61^{h}	84.57±0.60^{c}	10.10±0.34^{j}	5.33±0.6^{g}

The data are expressed as average value ± SD. Different letters in the same column indicate a significant difference ($P < 0.05$). RC, Relative crystallinity.

514 Table 2 T_2 relaxation time and in vitro digestibility of printed starch samples with different pre-
515 printing gelatinization degrees

Samples	RDS (%)	SDS (%)	RS (%)	T_{21}		T_{22}	
				Position (ms)	Percentage (%)	Position (ms)	Percentage (%)
RG-30	66.49±0.40^{k}	18.41±0.71^{b}	15.09±0.35^{a}	7.5	7.59±0.59^{a}	82.36	92.41±0.77^{h}
RG-40	70.45±0.66^{i}	17.50±0.79^{c}	12.05±0.62^{b}	6.72	7.33±0.49^{b}	94.1	92.67±0.66^{g}
RG-50	73.18±0.27^{h}	16.54±0.53^{d}	10.28±0.71^{c}	5.27	5.54±0.64^{d}	102.41	94.39±0.31^{h}
RG-60	77.45±0.37^{f}	14.30±0.31^{e}	8.25±0.78^{d}	3.41	6.04±0.59^{c}	112.82	93.96±0.77^{f}
RG-70	84.67±0.22^{d}	8.65±0.60^{h}	6.68±0.62^{e}	2.6	5.61±0.71^{d}	129.7	94.46±0.73^{e}
RG-100	92.47±0.25^{b}	5.64±0.34^{j}	1.89±0.36^{i}	-	-	-	-
WG-30	68.83±0.29^{j}	20.45±0.53^{a}	10.72±0.71^{c}	8.54	3.86±0.35^{f}	77.53	96.14±0.64^{c}
WG-40	74.11±0.39^{g}	17.21±0.41^{c}	8.68±0.72^{d}	6.65	3.35±0.31^{e}	82.39	96.65±0.67^{d}
WG-50	82.92±0.62^{e}	11.32±0.73^{f}	5.76±0.79^{f}	5.46	2.01±0.32^{g}	88.55	97.99±0.59^{b}
WG-60	86.17±0.36^{d}	9.32±0.32^{g}	4.51±0.48^{g}	3.62	1.83±0.73^{gh}	96.3	98.17±0.37^{ab}
WG-70	90.04±0.32^{c}	6.74±0.41^{i}	3.22±0.35^{h}	2.77	1.67±0.78^{i}	115.64	98.33±0.35^{a}
WG-100	93.83±0.43^{a}	4.65±0.57^{k}	1.52±0.53^{i}	-	-	-	-

516 The data are expressed as average value ± SD. Different letters in the same column indicate a significant
517 difference ($P < 0.05$). RDS, rapidly digestible starch; SDS, slowly digestible starch; RS, resistant starch.
518
519

Highlights

- ✓ Rice and wheat starches were processed by heat-extrusion 3D printing (HE-3DP)
- ✓ Pre-printing gelatinization degree affected starch printability and digestibility
- ✓ Ordered structure was induced with a low pre-printing gelatinization degree
- ✓ Crystallinity decreased as the pre-printing gelatinization degree increased
- ✓ Ideal printability and digestibility of rice and wheat starches were achieved

– Declaration of Interest –

Effect of pre-printing gelatinization degree on the starch structural evolution during hot-extrusion 3D printing and on digestibility

Bo Zheng [a], Yukuo Tang [a], Fengwei Xie [b]**, Ling Chen [a]*

[a] School of Food Science and Engineering, Guangdong Province Key Laboratory for Green Processing of Natural Products and Product Safety, Engineering Research Center of Starch and Vegetable Protein Processing Ministry of Education, South China University of Technology, Guangzhou 510640, China

[b] International Institute for Nanocomposites Manufacturing (IINM), WMG, University of Warwick, Coventry, CV4 7AL, United Kingdom

The authors declare that there is no conflict of interest regarding the publication of this article.